Proceedings of *RAGtime 23–25*
Z. Stuchlík, G. Török, V. Karas and D. Lančová, editors, Silesian University in Opava, 2023, pp. 151–166

Equilibrium tori orbiting Reissner-Nordström naked singularities

Ruchi Mishra[1,a] and Włodek Kluźniak[1]

[1]Nicolaus Copernicus Astronomical Center, Polish Academy of Sciences,
ul. Bartycka 18, 00-716 Warsaw, Poland
[a]rmishra@camk.edu.pl

ABSTRACT
In general relativity, the asymptotically flat space-time of a charged, spherically symmetric (non-rotating) body is described by the Reissner-Nordström metric. This metric corresponds to a naked singularity when the absolute value of charge, Q, exceeds the mass, M. For all Reissner-Nordström naked singularities, there exists a zero gravity sphere where a test particle can remain at rest. Outside that sphere, gravity is attractive, inside it, gravity is repulsive. For values of $Q/M > \sqrt{9/8}$, the angular frequency of circular test-particle orbits has a maximum at radius $r = (4/3)\,Q^2/M$. We construct polytropic tori with uniform values of specific angular momentum in the naked singularity regime of the Reissner-Nordström metric ($Q/M > 1$).

Keywords: Stars: gravity – naked singularities – accretion, accretion disks

INTRODUCTION

The gravity of a spherically symmetric, electrically charged body is described by the Reissner–Nordström (RN) space-time metric. For values of charge $Q > M$, the metric describes a naked singularity. One of the key features of many spherically symmetric naked singularities is the existence of a "zero-gravity" spherical surface, inside of which gravity is repulsive, whereas outside of it, gravity is attractive as usual (Pugliese et al., 2011; Vieira et al., 2014; Vieira and Kluźniak, 2023). This surface marks the innermost boundary for the existence of circular geodesics, representing orbits with zero angular momentum, a test particle remaining stably at rest there. In the RN case, no circular photon orbits exist for $Q/M > \sqrt{9/8}$. For a somewhat larger value still of Q/M, no marginally stable orbits exist, so test-particle circular orbits are stable all the way down to the zero-gravity sphere (Figure 1).

In a standard thin accretion disk, accretion is enabled by (effective) viscous torques transferring angular momentum outwards. This is possible as long as angular frequency decreases monotonically with the radius. In the case of RN space-time, the torque is reversed close to the zero-gravity radius, r_0, as $\mathrm{d}\Omega/\mathrm{d}r > 0$ there, for test particles. It is not yet clear whether a thin disk may exist all the way to the zero-gravity sphere. For this reason, we consider, instead, toroidal orbiting configurations of a perfect fluid.

978-80-7510-577-6

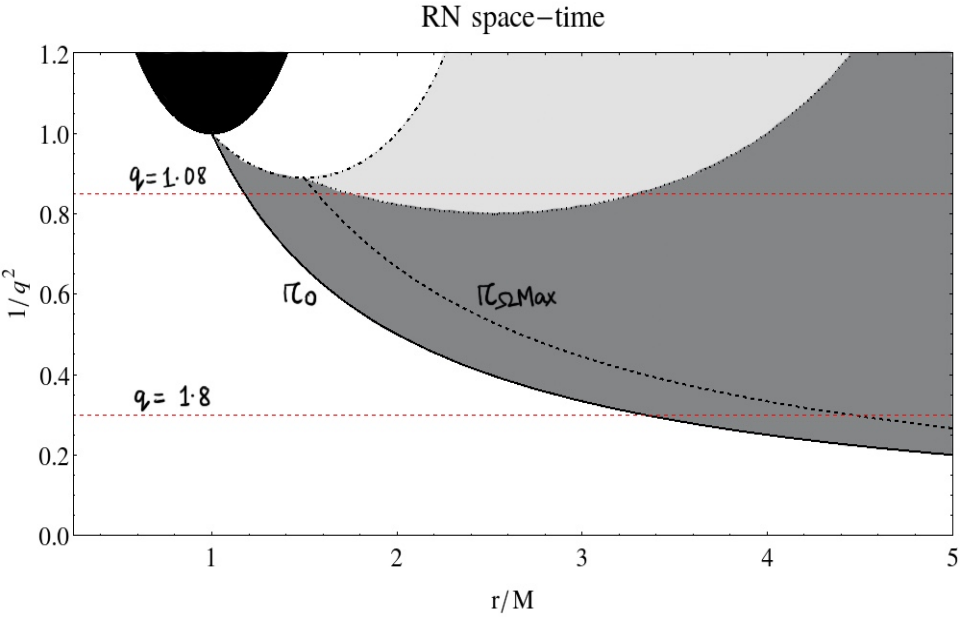

Figure 1. Orbital stability diagram for the RN spacetime ($q \equiv Q/M$). The *black* region corresponds to the hypervolume between the event horizons. The *solid black* line represents the zero gravity sphere (radius r_0). The *black dashed* lines represent the radius, $r_{\Omega\text{max}}$, at which angular frequency is maximum. The black *dotted* line corresponds to the marginally stable orbit, whereas the *dot-dashed* line corresponds to the photon orbit. *Dark grey* region corresponds to the stability region for time-like circular geodesics. *Light grey* region corresponds to the instability region for time-like circular geodesics. No circular geodesics exist in the *white* regions. The horizontal *red dashed* lines correspond to the two choices of Q/M ratio discussed in this contribution.

Here, we focus on the structure and shape[1] of equilibrium tori in which a perfect fluid is orbiting the RN naked singularity. As a first step, we consider uniform angular momentum distributions. Earlier work by Stuchlík et al. (2015); Kucáková et al. (2011); Prada-Méndez et al. (2023) presented the equilibrium toroidal structures in the case of Kehagias–Sfetsos naked singularities, Reissner-Nordström-(anti-)de Sitter space-times, and q-metric space-time respectively. Our results are qualitatively similar to Stuchlík et al. (2015). We use units with $G = 1, c = 1$. For convenience, since our results depend only on $(Q/M)^2$, we take $Q > 0$ to be the absolute magnitude of charge, the actual charge being $\pm Q$.

[1] While the configurations have the topology of a torus, their cross-section is not circular, not even ellipsoidal.

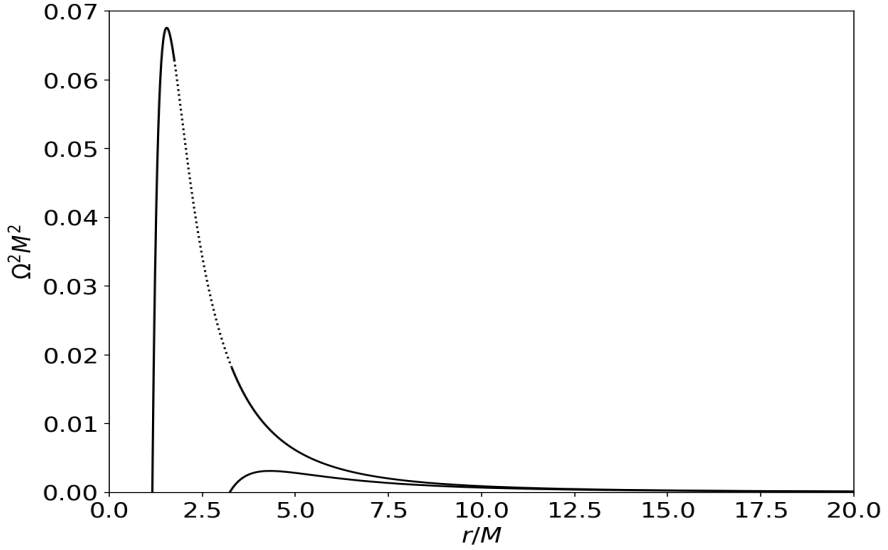

Figure 2. Square of orbital frequency as a function of r/M for charge value $Q/M = 1.08$ *(top)* and $Q/M = 1.8$ *(bottom).* The dotted line represents the unstable region.

GEODESIC MOTION IN RN SPACE TIME

The RN metric can be expressed in standard spherical coordinates as

$$\mathrm{d}s^2 = -f(r)\,\mathrm{d}t^2 + f^{-1}(r)\,\mathrm{d}r^2 + r^2\left(\mathrm{d}\theta^2 + \sin^2\theta\,\mathrm{d}\phi^2\right), \tag{1}$$

where $f(r)$ is the metric function given by

$$f(r) = 1 - \frac{2M}{r} + \frac{Q^2}{r^2}. \tag{2}$$

For a perfect fluid, the energy-momentum tensor is given by

$$T_{\mu\nu} = (p+\rho)\,u_\mu u_\nu - p g_{\mu\nu}, \tag{3}$$

where ρ is the fluid energy density and p its pressure. The four-velocity of the fluid in a circular orbit is $u^\mu = (u^t, 0, 0, u^\phi)$. The conserved energy and angular momentum of a test particle in this orbit are given by

$$E \equiv -g_{tt}\dot{t} = -u_t, \quad L \equiv g_{\phi\phi}\dot{\phi} = u_\phi. \tag{4}$$

The conserved specific angular momentum l is defined by

$$l \equiv \frac{L}{E} = -\frac{u_\phi}{u_t}. \tag{5}$$

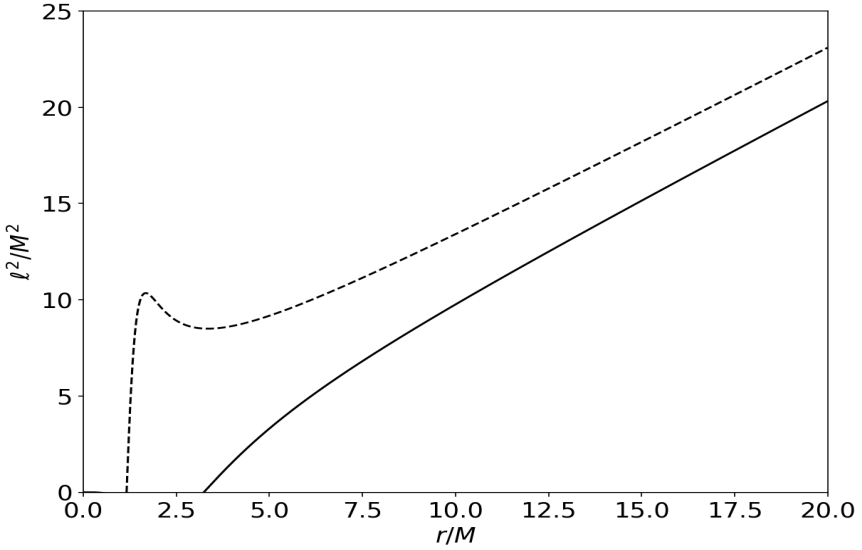

Figure 3. Square of specific angular momentum as a function of r/M for charge value $Q/M = 1.08$ (dashed) and $Q/M = 1.8$ (solid).

We begin with a discussion of test particle circular motion. The effective potential can be conveniently taken to be E^2, in the equatorial plane ($\sin\theta = 1$) it reduces to

$$V_{\rm eff}\,(r) = f\,(r)\left(1 + \frac{L^2}{r^2}\right), \tag{6}$$

where we've used $u_\mu u^\mu = -1$. The condition $\partial V_{\rm eff}/\partial r = 0$ then gives the angular momentum of circular geodesics, i.e.

$$L^2\,(r) = \frac{r^3 f'\,(r)}{2f - rf'\,(r)}, \tag{7}$$

or

$$l^2\,(r) = \frac{r^3}{2f^2} f'\,(r)\,. \tag{8}$$

The orbital angular frequency, $\Omega = u^\phi/u^t$, so

$$\Omega^2\,(r) = \frac{f'\,(r)}{2r}. \tag{9}$$

The angular velocity for two values of Q/M is illustrated in Figure 2.

For the RN space-time, the maximum angular velocity is given by the condition

$$\frac{\mathrm{d}\Omega^2}{\mathrm{d}r^2} = \frac{\mathrm{d}}{\mathrm{d}r}\left(\frac{f'(r)}{2r}\right) = 0, \tag{10}$$

so the maximum of angular velocity occurs at

$$r_{\Omega\mathrm{max}} = \frac{4}{3}\frac{Q^2}{M}. \tag{11}$$

In Figure 2 we present this radius, $r_{\Omega\mathrm{max}}$ as a function of Q/M. As circular geodesics are not possible within the photon orbit, $r_{\Omega\mathrm{max}}$ is only defined as long as $Q/M > \sqrt{9/8}$. Note that the marginally orbits, when they exist, are always at a larger radius – the maximum of Ω is always attained in a stable orbit. The specific angular momentum at this orbit (of maximum Ω) is given by,

$$l_{\Omega\mathrm{max}} \equiv l(r_{\Omega\mathrm{max}}). \tag{12}$$

It is interesting to note that the specific angular momentum and its radial derivative in circular orbits are not necessarily monotonic as a function of the radius r. The extrema of the $l(r)$ curve (if present) corresponds to the marginally stable orbits. The region between the maximum and minimum of the $Q/M = 1.08$ specific angular momentum curve in Figure 3 correspond to unstable circular orbits (c.f. Figure 2) by Rayleigh's criterion, as $\mathrm{d}l/\mathrm{d}r < 0$ there.

In the case of barotropic fluid, the surfaces of constant pressure (isobars) corresponding to equipotential surfaces $W(r,\theta)$ are given by Boyer's condition (e.g., Abramowicz et al., 1978; Kozlowski et al., 1978)

$$-\int_0^p \frac{\mathrm{d}p}{p+\rho} = W - W_{\mathrm{in}} = \ln\frac{u_t}{(u_t)_{\mathrm{in}}} - \int_{l_{\mathrm{in}}}^{l}\frac{\Omega \mathrm{d}l}{1-\Omega l}. \tag{13}$$

In the Newtonian limit, W is the usual effective potential. Here, the subscript "in" refers to the inner edge of the torus. The equipotential surfaces are determined by the condition

$$W(r,\theta) = \text{constant}. \tag{14}$$

For the simplest case of tori with uniform distribution of specific angular momentum, $l_0(r,\theta) = \text{constant}$, W is given by the following equation (Rezzolla and Zanotti, 2013):

$$W(r,\theta) = \ln|u_t| = \frac{1}{2}\ln\left[\frac{f(r)\,r^2\sin^2\theta}{r^2\sin^2\theta - f(r)\,l_0^2}\right].$$

At a given point in the (r,θ) plane, the potential W can be positive or negative, indicating open and closed equipotential surfaces. In principle, the fluid can fill any of the closed surfaces. Thus, a closed equipotential surface can be taken to represent the surface of

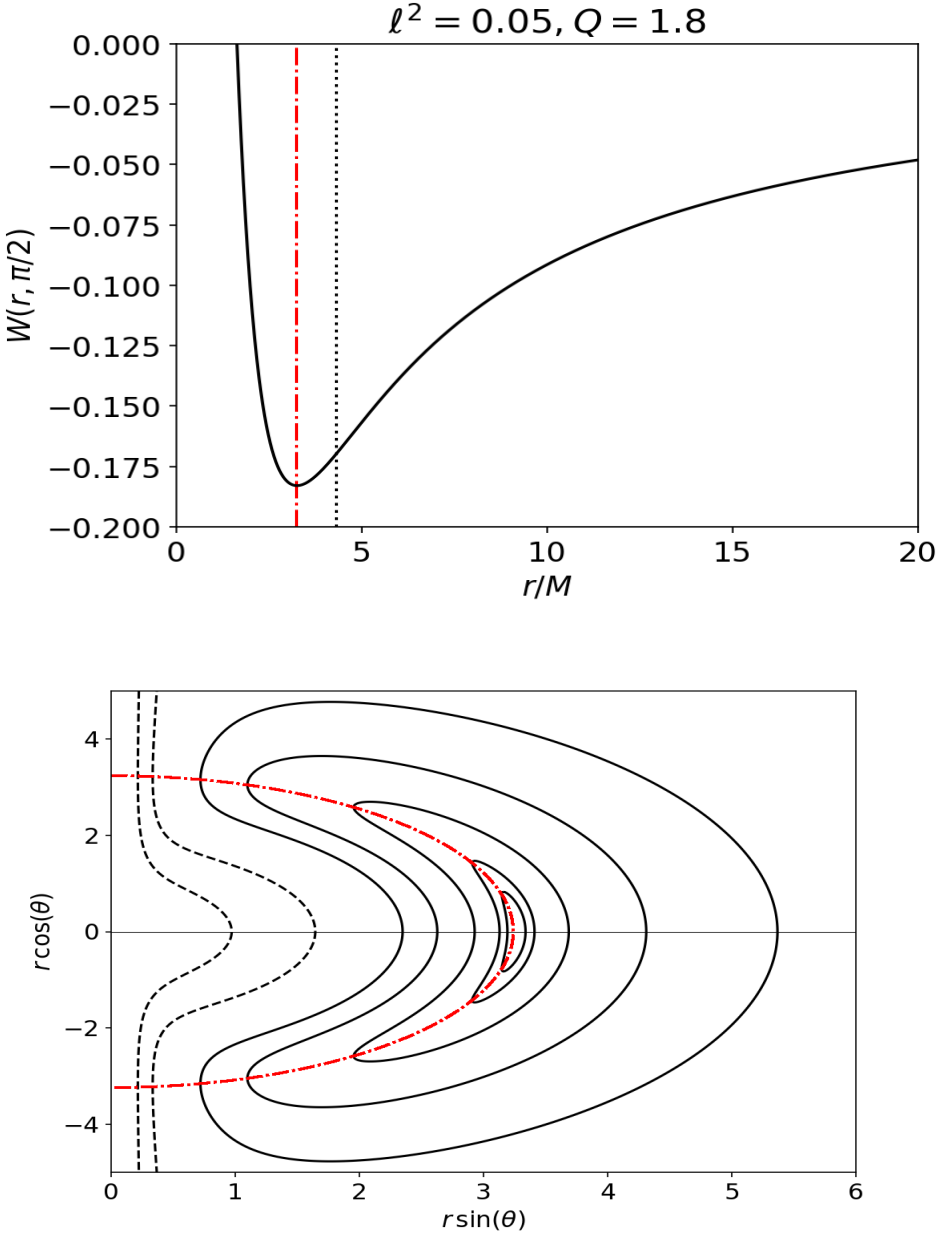

Figure 4. Equilibrium tori around RN naked singularity with Q/M=1.8 with $l_0 < l_{\Omega\max}$. Location of the zero-gravity sphere is indicated by red dotted-dashed line. *Top:* W as a function of r/M in equatorial plane. The radius of maximum angular frequency, $r_{\Omega\max}$, is indicated by the black dotted line. *Bottom:* Meridional cross-section of the equipotential surfaces. Solid closed lines represent toroidal surfaces with negative W value. The black dashed lines represent positive values of W.

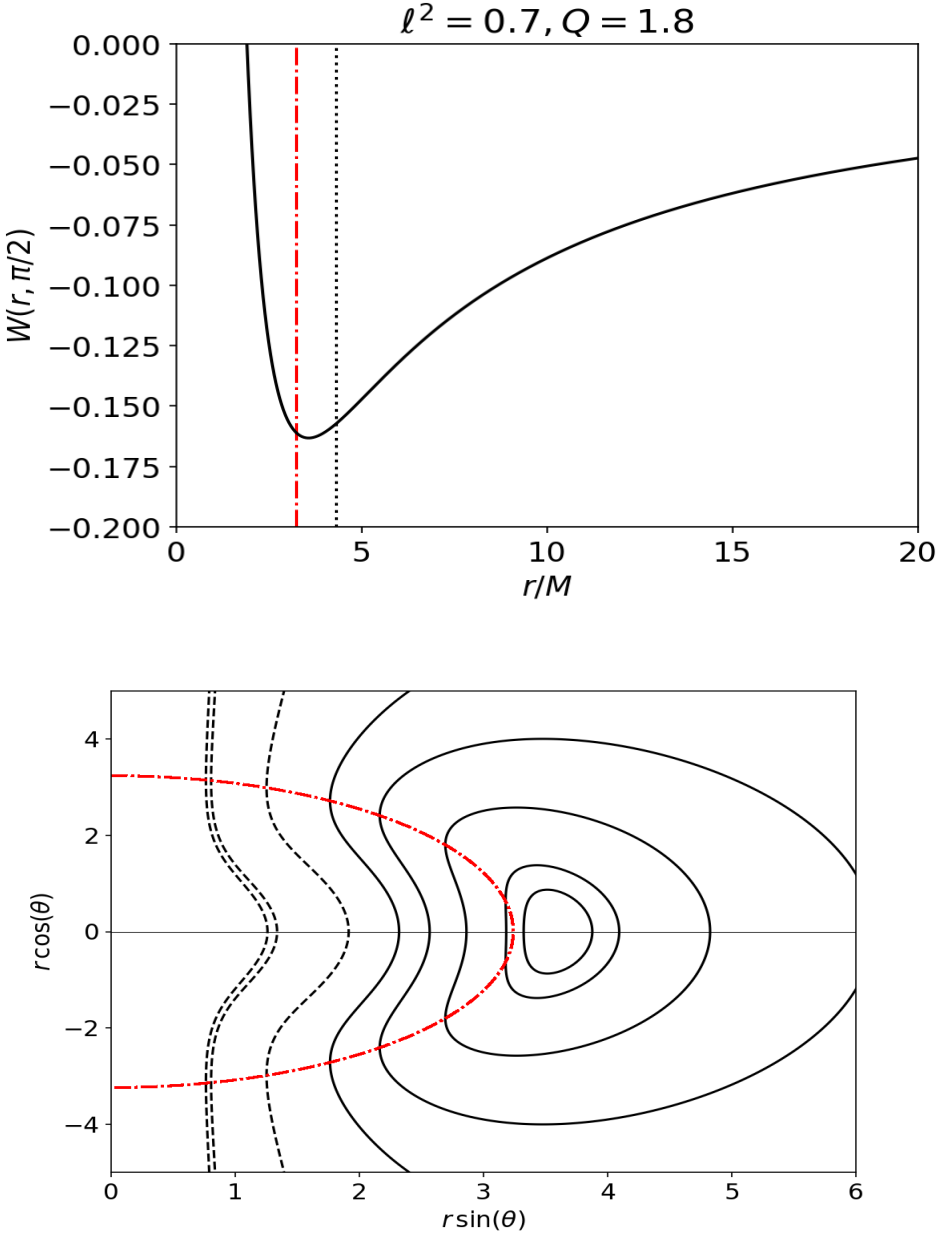

Figure 5. Equilibrium tori around RN naked singularity with Q/M=1.8 with $l_0 < l_{\Omega\max}$. Location of the zero-gravity sphere is indicated by red dotted-dashed line. *Top:* W as a function of r/M in equatorial plane. The radius of maximum angular frequency, $r_{\Omega\max}$, is indicated by the black dotted line. *Bottom:* Meridional cross-section of the equipotential surfaces. Solid closed lines represent toroidal surfaces with negative W value. The black dashed lines represent positive values of W.

a stationary configuration of orbiting fluid. The pressure of the toroidal barytrope is zero at the surface, with a non-zero gradient.

For RN naked singularity for constant specific angular momentum l_0, the potential W takes the following form:

$$W(r,\theta) = \ln|u_t| = \frac{1}{2}\ln\left[\frac{(r^2 - 2Mr + Q^2)\sin^2\theta}{r^2\sin^2\theta - (r^2 - 2Mr + Q^2)l_0^2/r^2}\right]. \tag{15}$$

TOROIDAL PERFECT FLUID CONFIGURATIONS

We construct equilibrium toroidal configurations for four representative values of the angular momentum parameter, l_0, for each of two values of the charge-to-mass ratio (Table 1). These are shown with solid lines in Figs. 4–11. The dashed lines correspond to the surfaces with positive values of W in Eq. (15), so any fluid in their vicinity would be unbound.

The barotropic fluid was assumed to have a uniform distribution of angular momentum. Let us start by discussing the case of $Q/M = 1.8$, representative of singularities with no marginally stable orbits. For low values of specific angular momentum, the circular locus of maximum pressure in the torus (the torus "center") lies very close to the zero-gravity sphere. While the torus can penetrate the zero-gravity sphere, its gradient of pressure balancing the repulsive gravity, a large part of the fluid must necessarily orbit outside of the zero-gravity sphere. The gravitational repulsion of the naked singularity leads to a very distorted shape of the "torus," which by analogy to, and in contrast with, the well-known black hole "cusp" solution[2] (known informally as "Sikora's beak") could best be described as open "jaws" ready to snatch the singularity (Figure 4). For solutions with larger values of angular momentum, these jaws become less prominent and finally disappear as the center of the torus shifts outwards with increasing angular momentum parameters (Figures 4–7).

For low values of the charge-to-mass ratio, the presence of marginally stable orbits complicates the solutions. Here, we discuss $Q/M = 1.08$ as an example. For low values of angular momentum, the jaws are again apparent inside the zero-gravity sphere (Figure 8). However, for larger values of angular momentum, the torus ends close to the zero-gravity sphere, as though it hit a wall (Figure 9). For larger values of l_0 still, two separate toroidal solutions appear (Figure 10). This is related to the two stable orbital solutions for a test particle for a certain range of specific angular momenta (e.g., values of l_0 near the maximum of the dashed line in Figure 3). Once angular momentum exceeds the maximum of the $l(r)$ curve, only one stable orbital solution exists at large radii, and the fluid configuration adopts the shape familiar from studies of compact object gravity in the quasi-Newtonian regime, i.e., far from the source of gravity (Figure 11).

[2] Introduced for the first time in Abramowicz, Jaroszyński & Sikora 1978.

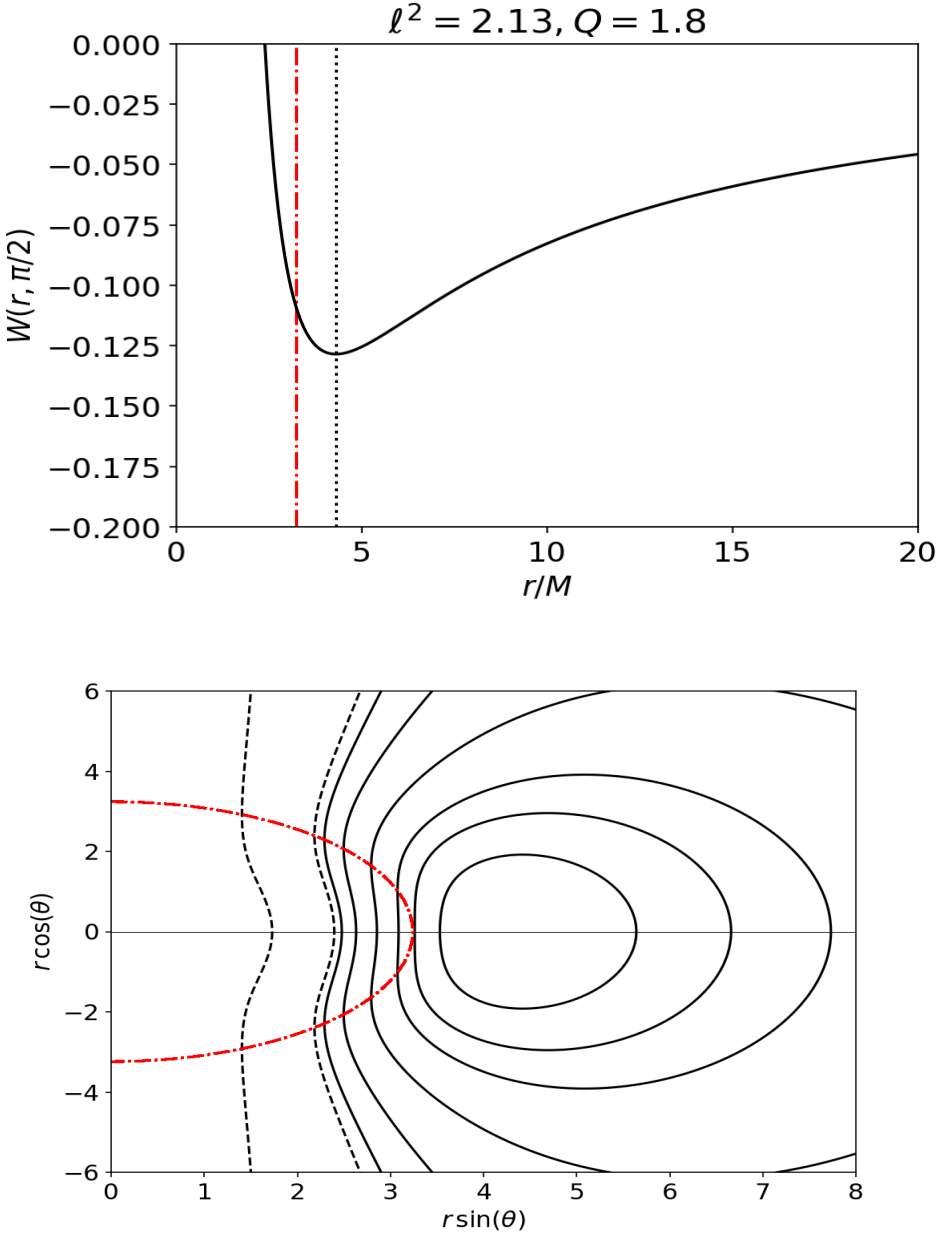

Figure 6. Equilibrium tori around RN naked singularity with Q/M=1.8 with $l_0 = l_{\Omega\max}$. Location of the zero-gravity sphere is indicated by red dotted-dashed line. *Top:* W as a function of r/M in equatorial plane. The radius of maximum angular frequency, $r_{\Omega\max}$, is indicated by the black dotted line. *Bottom:* Meridional cross-section of the equipotential surfaces. Solid closed lines represent toroidal surfaces with negative W value. The black dashed lines represent positive values of W.

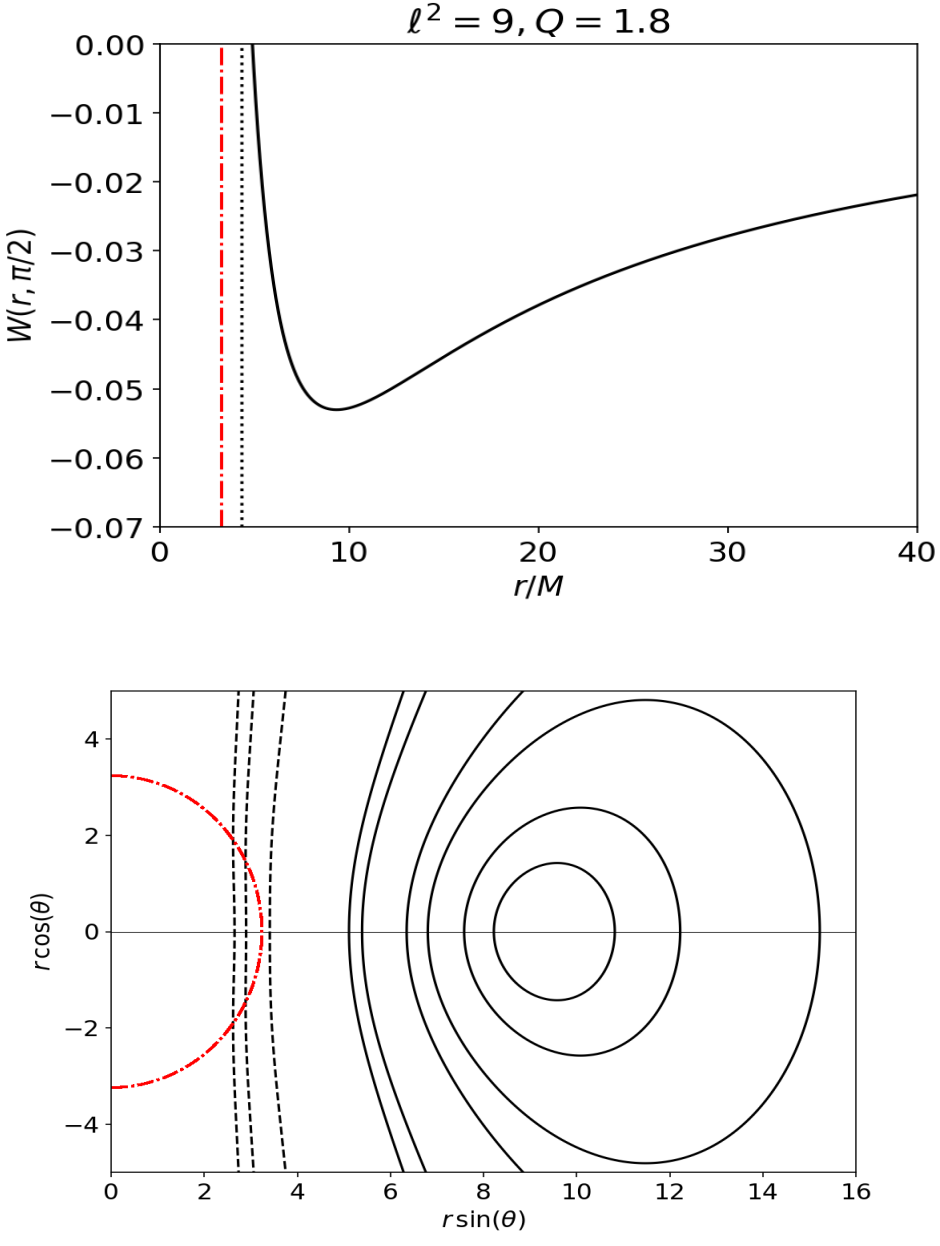

Figure 7. Equilibrium tori around RN naked singularity with Q/M=1.8 with $l_0 > l_{\Omega\max}$. Location of the zero-gravity sphere is indicated by red dotted-dashed line. *Top:* W as a function of r/M in equatorial plane. The radius of maximum angular frequency, $r_{\Omega\max}$, is indicated by the black dotted line. *Bottom:* Meridional cross-section of the equipotential surfaces. Solid closed lines represent toroidal surfaces with negative W value. The black dashed lines represent positive values of W.

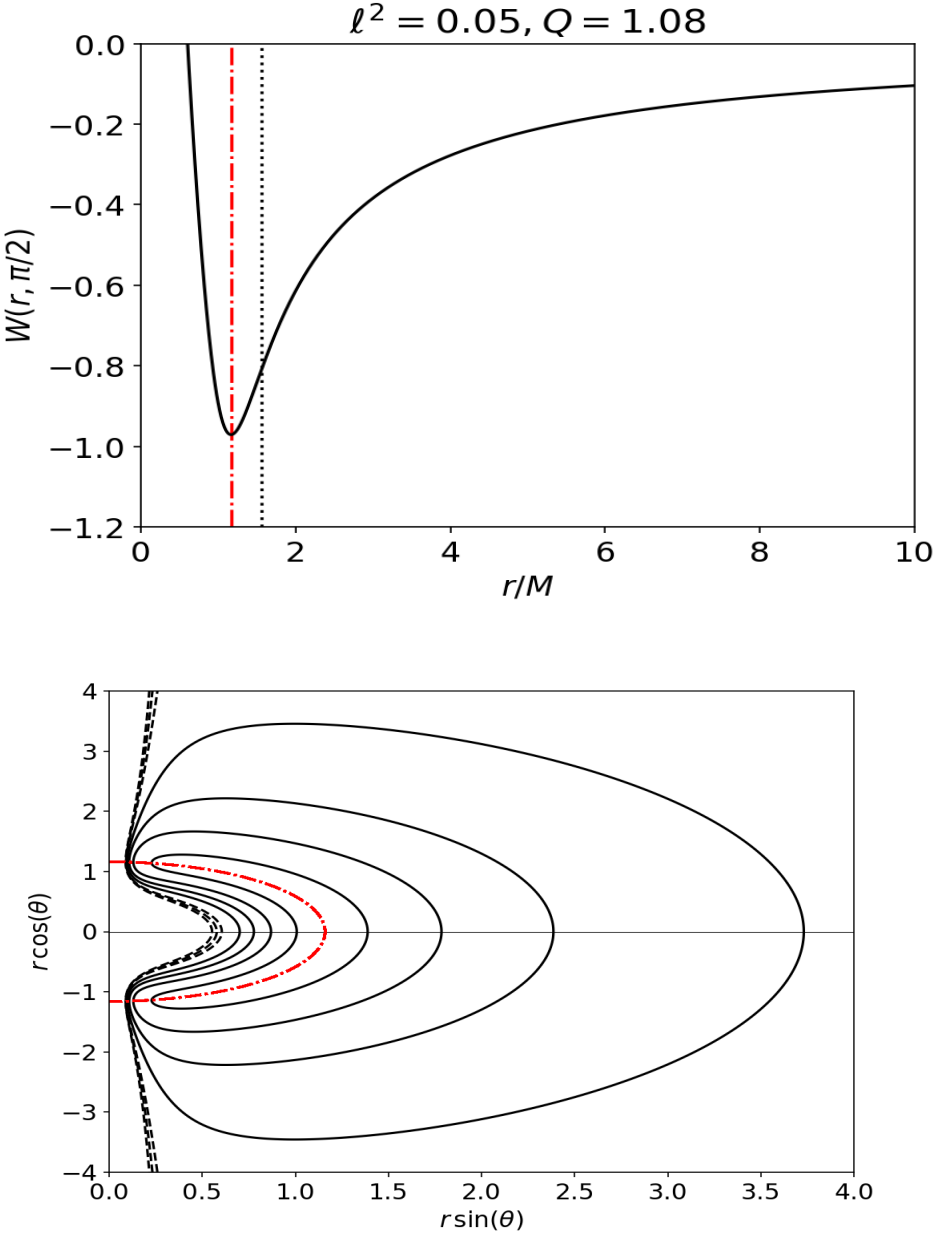

Figure 8. Equilibrium tori around RN naked singularity with Q/M=1.8 with $l_0 < l_{\Omega\max}$. Location of the zero-gravity sphere is indicated by red dotted-dashed line. *Top:* W as a function of r/M in equatorial plane. The radius of maximum angular frequency, $r_{\Omega\max}$, is indicated by the black dotted line. *Bottom:* Meridional cross-section of the equipotential surfaces. Solid closed lines represent toroidal surfaces with negative W value. The black dashed lines represent positive values of W.

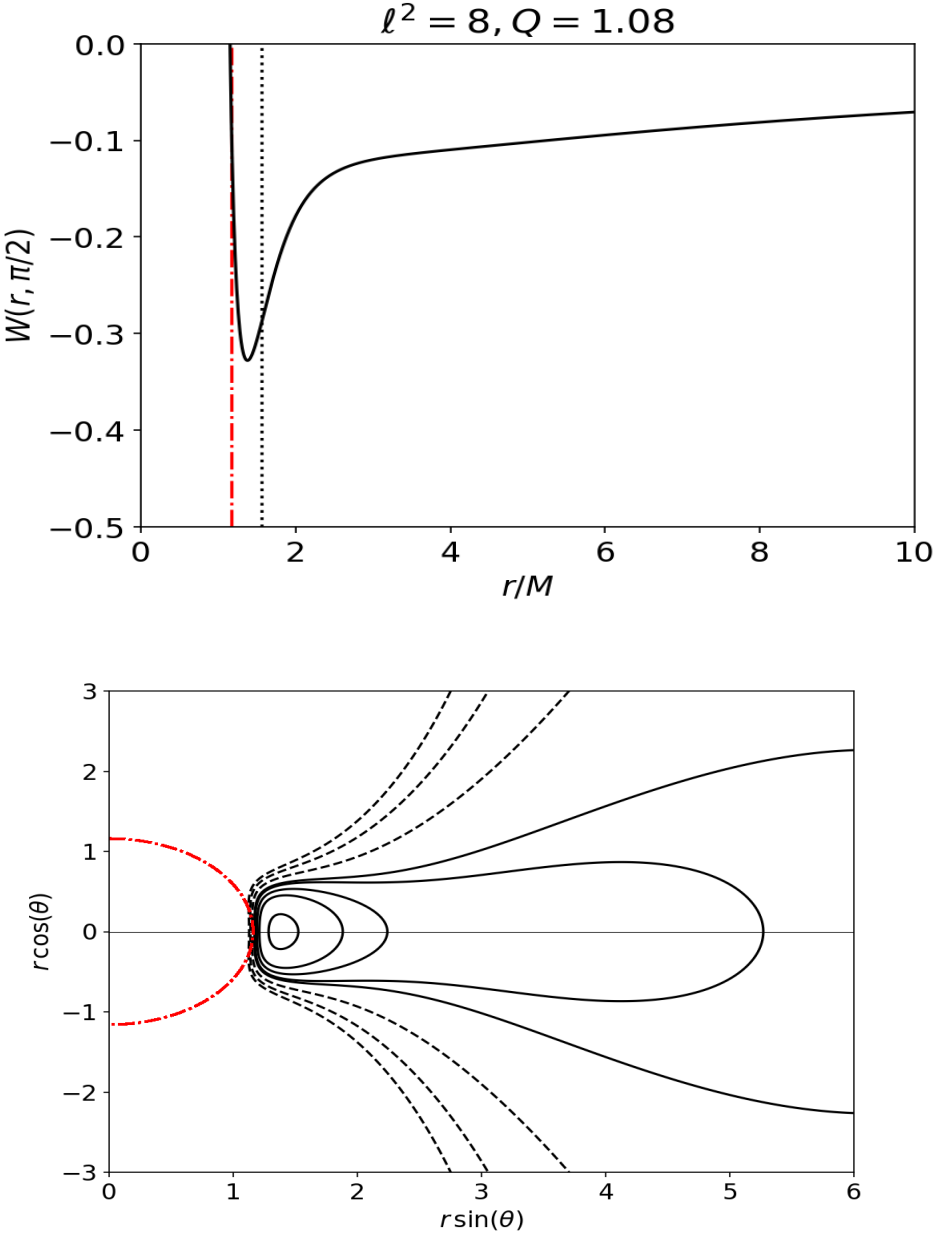

Figure 9. Equilibrium tori around RN naked singularity with Q/M=1.8 with $l_0 < l_{\Omega\max}$. Location of the zero-gravity sphere is indicated by red dotted-dashed line. *Top:* W as a function of r/M in equatorial plane. The radius of maximum angular frequency, $r_{\Omega\max}$, is indicated by the black dotted line. *Bottom:* Meridional cross-section of the equipotential surfaces. Solid closed lines represent toroidal surfaces with negative W value. The black dashed lines represent positive values of W.

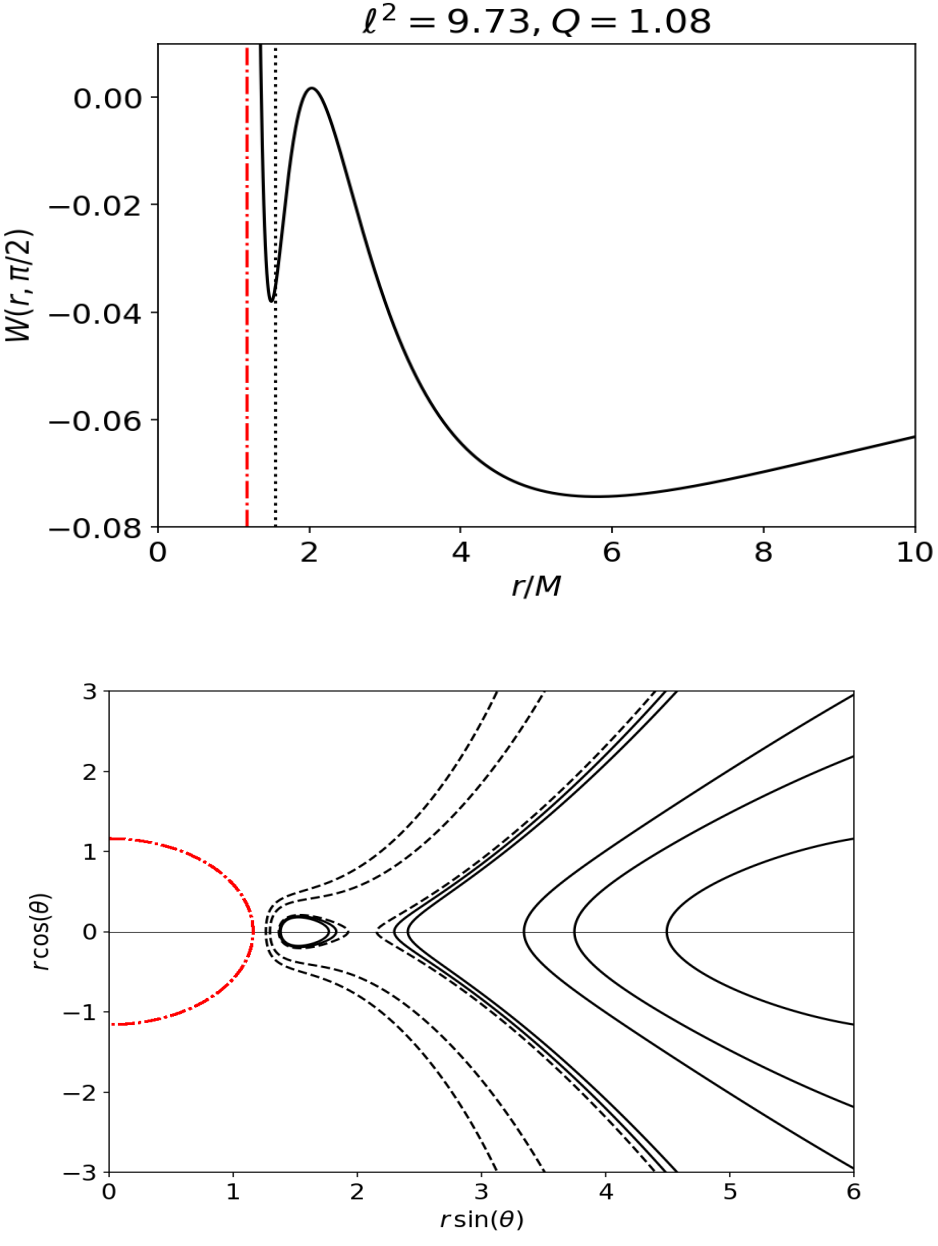

Figure 10. Equilibrium tori around RN naked singularity with Q/M=1.8 with $l_0 = l_{\Omega\max}$. Location of the zero-gravity sphere is indicated by red dotted-dashed line. *Top:* W as a function of r/M in equatorial plane. The radius of maximum angular frequency, $r_{\Omega\max}$, is indicated by the black dotted line. *Bottom:* Meridional cross-section of the equipotential surfaces. Solid closed lines represent toroidal surfaces with negative W value. The black dashed lines represent positive values of W.

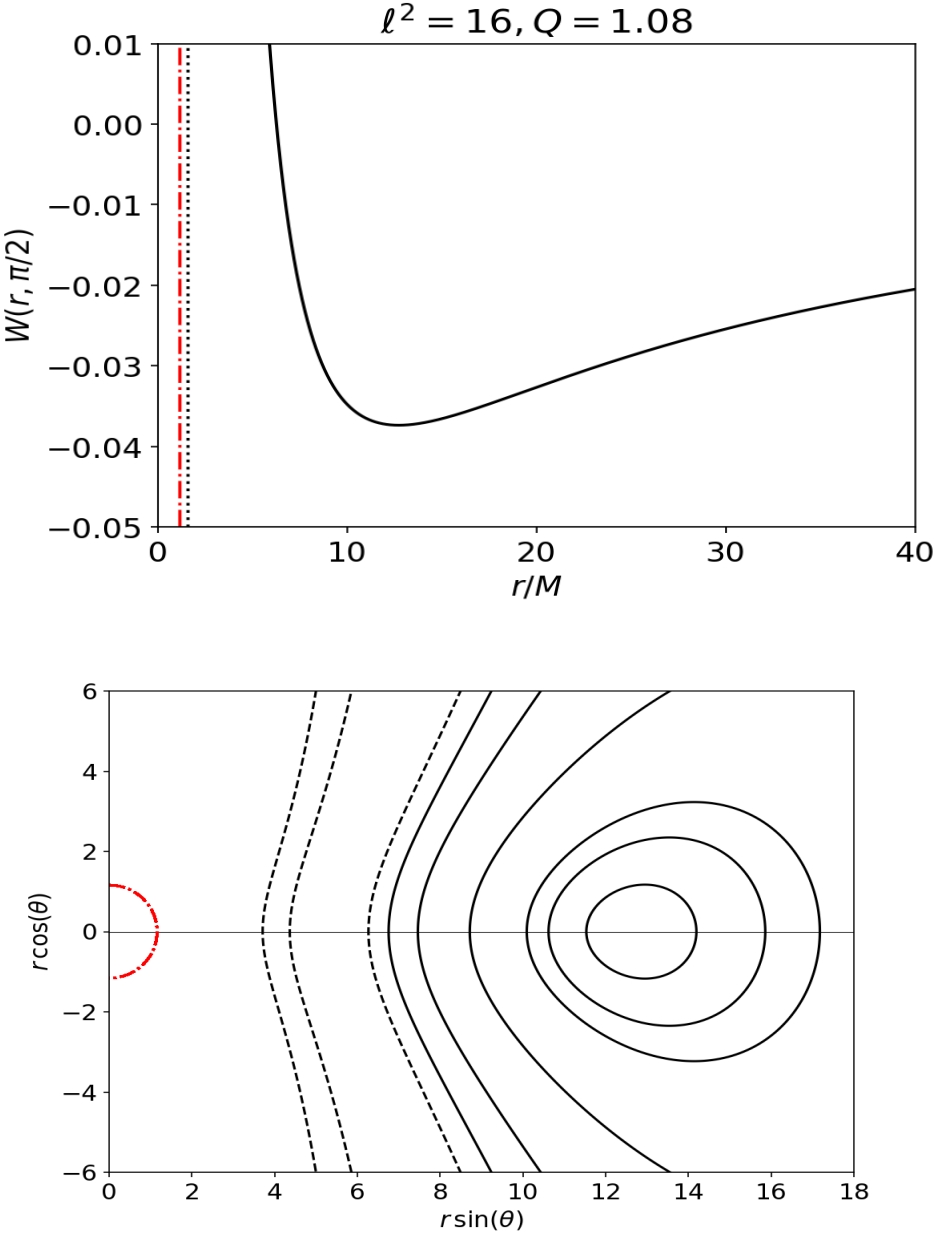

Figure 11. Equilibrium tori around RN naked singularity with Q/M=1.8 with $l_0 > l_{\Omega\max}$. Location of the zero-gravity sphere is indicated by red dotted-dashed line. *Top:* W as a function of r/M in equatorial plane. The radius of maximum angular frequency, $r_{\Omega\max}$, is indicated by the black dotted line. *Bottom:* Meridional cross-section of the equipotential surfaces. Solid closed lines represent toroidal surfaces with negative W value. The black dashed lines represent positive values of W.

Q/M	$l_0^2 << (l_{\Omega\max})^2$	$l_0^2 < (l_{\Omega\max})^2$	$l_0^2 = (l_{\Omega\max})^2$	$l_0^2 > (l_{\Omega\max})^2$
1.08	0.05	8	9.73	16
1.8	0.05	0.7	2.13	9

Table 1. List of specific angular momentum values used in our calculations for two different charge to mass ratios.

CONCLUSIONS

We have studied the shape of fluid tori orbiting the RN naked singularities. Historically, such studies were performed for black holes to gather insight into accretion disks in an era before numerical simulations were feasible. This is the first step of a program aiming to retrace this historical development for the case of naked singularities.

We consider perfect fluid configurations in hydrostatic equilibrium with non-zero[3] uniform angular momentum orbiting Reissner-Nordström singularities. We find that typically, no cusp is formed at the inner edge of toroidal figures of equilibrium around RN singularities. A toroidal solution with a cusp (on the inside of the outer torus or on the outside of the inner torus) can at most be found in that narrow charge-to-mass ratio parameter when marginally stable orbits exist (Figure 10). Unlike in black holes, the equipotential surfaces in RN singularities never self-intersect. Thus, unlike in black holes, where accretion from a toroidal “disk" may proceed onto the compact object through “Roche-lobe-like" overflow with no angular momentum loss, the RN singularity can only be approached if the accreting fluid loses its excess angular momentum—the zero-gravity sphere is engulfed by the fluid only at low values of specific angular momentum (e.g., Figures 4-6). At higher values of specific angular momentum, only unbound matter may approach the singularity (or even the zero-gravity sphere), but it is likely to outflow to infinity (e.g., Figure 7).

The positions and shapes of the constant specific angular momentum equilibrium tori may also be taken to illustrate the general conclusion that for the Reissner-Nordström naked singularity (and similar space-times), a part of any figure of equilibrium of an orbiting fluid must always lie outside of the zero gravity sphere. This may have applications in interpreting the Event Horizon Telescope (EHT) observations of the center of our Galaxy (Mishra and Vieira, 2023).

ACKNOWLEDGEMENTS

This work was supported in part by the Polish NCN grant 2019/33/B/ST9/01564.

[3] The zero-angular momentum configurations (levitating atmospheres) are discussed in Vieira and Kluźniak (2023)

REFERENCES

Abramowicz, M., Jaroszynski, M. and Sikora, M. (1978), Relativistic, accreting disks., *Astron. Astrophys*, **63**, pp. 221–224.

Kozlowski, M., Jaroszynski, M. and Abramowicz, M. A. (1978), The analytic theory of fluid disks orbiting the Kerr black hole., *Astron. Astrophys*, **63**(1-2), pp. 209–220.

Kucáková, H., Slaný, P. and Stuchlík, Z. (2011), Toroidal configurations of perfect fluid in the Reissner-Nordström-(anti-)de Sitter spacetimes, *J. Cosmol. Astropart. Phys.*, **2011**(1), 033.

Mishra, R. and Vieira, R. S. S. (2023), Conservative limits on the electric charge of Sgr A* in the Reissner-Nordstrom metric, *arXiv e-prints*, arXiv:2304.04313, arXiv: 2304.04313.

Prada-Méndez, G. D., Lora-Clavijo, F. D. and Velásquez-Cadavid, J. M. (2023), Synchrotron emitting Komissarov torus around naked singularities, *Classical and Quantum Gravity*, **40**(19), 195011, arXiv: 2308.09174.

Pugliese, D., Quevedo, H. and Ruffini, R. (2011), Circular motion of neutral test particles in Reissner-Nordström spacetime, *Phys. Rev.D*, **83**(2), 024021, arXiv: 1012.5411.

Rezzolla, L. and Zanotti, O. (2013), *Relativistic Hydrodynamics*.

Stuchlík, Z., Pugliese, D., Schee, J. and Kučáková, H. (2015), Perfect fluid tori orbiting Kehagias-Sfetsos naked singularities, *European Physical Journal C*, **75**, 451, arXiv: 1412.4149.

Vieira, R. S. S. and Kluźniak, W. (2023), Astrophysical cloaking of a naked singularity, *Monthly Notices of the Royal Astronomical Society*, **523**(3), pp. 4615–4623, ISSN 0035-8711, URL https://doi.org/10.1093/mnras/stad1718.

Vieira, R. S. S., Schee, J., Kluźniak, W., Stuchlík, Z. c. v. and Abramowicz, M. (2014), Circular geodesics of naked singularities in the kehagias-sfetsos metric of hořava's gravity, *Phys. Rev. D*, **90**, p. 024035.